行政院國家科學委員會專題研究計畫　成果報告

在豬隻心房顫動模式中功能性基因體的變化(3/3)

計畫類別：個別型計畫
計畫編號：NSC93-2314-B-002-014-
執行期間：93 年 08 月 01 日至 94 年 07 月 31 日
執行單位：國立臺灣大學醫學院內科

計畫主持人：賴凌平

報告類型：完整報告

處理方式：本計畫可公開查詢

中　華　民　國 94 年 10 月 21 日

行政院國家科學委員會補助專題研究計畫 ☑ 成 果 報 告
□期中進度報告

在豬隻心房顫動模式中功能性基因體的變化

(3/3)

計畫類別：☑ 個別型計畫　　□ 整合型計畫
計畫編號：NSC 93－2314－B－002－014－
執行期間：　93 年 8 月 1 日至 94 年 7 月 31

計畫主持人：賴凌平
共同主持人：
計畫參與人員：

成果報告類型(依經費核定清單規定繳交)：□精簡報告　☑完整報告

本成果報告包括以下應繳交之附件：
□赴國外出差或研習心得報告一份
□赴大陸地區出差或研習心得報告一份
□出席國際學術會議心得報告及發表之論文各一份
□國際合作研究計畫國外研究報告書一份

處理方式：除產學合作研究計畫、提升產業技術及人才培育研究計畫、列管計畫及下列情形者外，得立即公開查詢
□涉及專利或其他智慧財產權，□一年□二年後可公開查詢

執行單位：國立臺灣大學醫學院內科

中　華　民　國　94　年　10　月　20　日

中文摘要及關鍵詞

前言：

在心房顫動的過程中，心房組織會發生功能性以及結構性的改變，而這些改變又會造成心房顫動的進一步惡化，因此我們利用 cDNA 微陣列以及二維蛋白電泳的方式，以期找出心房顫動時，心房組織的變化。

方法及結果：

我們首先在豬隻建立一個心房顫動的模式，而其方法是以右心房每分鐘 600 次的電刺激而造成。在心房快速刺激六星期後，將豬隻犧牲並取得心房組織，接著我們使用含有 6035 個 cDNA 的微陣列來研究 mRNA 的變化，再以二維電泳的方式來研究蛋白的變化。在 cDNA 微陣列的實驗中，我們發現在左心房中 387 個基因有明顯的變化，而在右心房中有 81 個基因有明顯的變化，在這些基因中，以 MLC-2V 的變化最大，在左心房中達 9.4 倍上升，而在右心房中達 7.3 倍上升，在二維蛋白電泳中，我們發現在 pI 4.5 到 5.0 之間，18-20kd 的位置有三個蛋白點有明顯上升。經由進一步質譜分析發現，這三個蛋白點都是 MLC-2V，而與 mRNA 的變化相符合。

結論：

cDNA 微陣列及二維蛋白電泳都顯示，心房顫動時，心房組織會產生特異性的變化，而其中 MLC-2V 的上升是典型的變化。

英文摘要及關鍵詞(keywords)

Abstract

Introduction Functional and structural changes of the atrial tissue occur during the natural course of Af and these changes may contribute to further Af. We investigated the changes in atrial fibrillation (Af) tissue using cDNA microarray and two-dimensional protein electrophoresis techniques.

Methods and Results We established a porcine model of Af by rapid right atrial appendage pacing at a rate of 600/min. Atrial tissue was obtained after rapid atrial depolarization for 6 weeks. Microarrays containing 6035 cDNA clones were used to evaluate the alterations of mRNA while two-dimensional protein electrophoresis was performed to compare protein patterns. In cDNA microarray studies, we identified 387 genes with significant change in the left atrium and 81 genes in the right atrium. Among the genes, the ventricular isoform of the myosin regulatory light chain (MLC-2V) showed the greatest fold of change (9.4 and 7.3 in the left and right atrium respectively). In protein electrophoresis, the expression levels of three protein spots spanning from 18 to 20 Kd in the acidic region (PI 4.5 to 5.0) were specifically elevated in the Af group. Interestingly, through tandem mass spectrometric analysis, these three spots were identified to be MLC-2V. Thus MLC-2V expression at the mRNA and protein levels corresponded well and both indicated a significant increase in Af.

Conclusions Both cDNA microarray and 2D-PAGE studies revealed characteristic

changes in Af tissue. We demonstrated the re-programming of myosin regulatory light chain isoform composition with a significant increase of its ventricular isoform (MLC-2V).

Key words atrial fibrillation, cDNA microarray, 2-D PAGE, mass spectrometry, myosin regulatory light chain

Introduction

Atrial fibrillation (Af) is the most common tachyarrhythmia in humans. There is evidence showing that Af begets Af and through this vicious cycle Af becomes incessant.[1] During the natural course of Af, atrial myocytes undergo functional as well as structural changes and these changes contribute to further Af. Among these changes, alterations in gene expression with subsequent changes in protein levels are a common way of adaptation to stress conditions. Past studies also showed that there are changes at mRNA and protein levels of ion channels, calcium handling proteins, receptors and so on.[2-5] However, most studies focused only on a limited number of selected candidate genes. In the present study, we investigated the alterations of mRNAs and proteins from a global point of view. For changes in mRNA levels, cDNA microarray techniques were used to screen thousands of genes. For changes in protein levels, two-dimensional protein electrophoresis techniques as well as mass spectrometric analysis were applied. With these techniques, we were able to screen the changes of thousands of genes in Af tissue in genomic and proteomic views.[6-7]

Materials and Methods

Porcine model of Af

The porcine model of atrial fibrillation has been reported in detail previously.[8] In total, there were twelve adult pigs of Yorkshire-Landrace strain used (6 in the Af group and 6 in the control group). The initial body weight was 65 ± 13 kg (range 50 to

81 kg). Under intravenous anesthesia by thiamylal (2-3 mg/kg) (Kyorin Pharmaceutical Co., Tochigi, Japan), all animals were transvenously implanted with a high-speed pacemaker (Itrel-III, Medtronic, Minneapolis, MN, USA). The pacemaker was pacing the atria at a rate of 600 beats per minute in the Af group for four weeks. After four weeks of continuous pacing, the atrial pacemaker was turned off and the pigs were in Af. The pigs were sacrificed 2 weeks after turning of the pacemaker and the total duration of rapid atrial depolarization was 6 weeks. For the control group, the pacemaker remained off for 6 weeks after the implantation. Transmural tissue blocks were obtained from the right atria free wall and left atrial free wall.

RNA isolation

Total cellular RNA extraction was performed immediately after obtaining the atrial tissue. The tissue was homogenized with a Polytrone-Aggregate (Dispergier-und Mischtechnik, Switzerland) and Trizol solution (Gibco BRL, Grand Island, NY, USA) was added for RNA extraction.

DNA microarray experiments

Fluorescently labeled cDNA probes were generated by reverse transcription of total cellular RNA isolated from Af or control atrial tissue in the presence of Cy5 or Cy3 dCTP respectively (Amersham, Piscataway, NJ, USA). The probes were applied to microarrays containing 6035 human cDNA clones (UniversoChip, AsiaBioinnovations Corporation, Newark, CA, USA) for hybridization. The intensities of hybridization were measured by sequential excitation of the two

fluorophores with a scanning laser read at wavelength of 635nm (for Cy5) and 525nm (for Cy3) respectively.

Two-dimensional polyacrylamide protein electrophoresis (2D-PAGE)

Left atrial tissue was lyophilized for 48 hours and then crushed in a mortar containing liquid nitrogen. One mg tissue power was homogenized in a 200μl sample buffer (7 urea, 2M thiourea, 4% CHAPS, 65mM DTT). Isoelectric focusing was performed using immobilized pH gradient strips (Pharmacia, Uppsala, Sweden), which had a pH range 4~7. A gradient of 300-3500 V was applied to the strips followed by constant 3500 V, with focusing complete after 120KVh. Equilibrated strips were inserted onto a 9~16% vertical gradient SDS-PAGE for 5 hours at 20 mA/gel for second dimension separation. After electrophoresis, the gel was silver stained. The image was scanned and analyzed using Melanie III (GeneBio, Geneva, Switzerland). Parallel gels were silver stained in the absence of glutaraldehyde for further mass spectrometric analysis.

Mass spectrometry (MS) analysis

The excised gel pieces were first destained in the destaining solution containing 15 mM potassium ferricyanide and 50 m sodium thiosulfate. After washing in 25 mM NH_4HCO_3, the gels were subjected to reduction, pyridylethylation and tryptic digestion as described by Tsay et al.[9] Multiple peptide sequences were determined in a single run by capillary reverse phase chromatography directly coupled to a liquid chromatography quadruple ion trap mass spectrometer (Thermo Finnigan, San Jose,

CA, USA) equipped with a standard electrospray source. The ion trap MS was programmed to acquire three successive scan modes consisting of full-scan MS over the range 395-1650 m/z, followed by two data-dependent scans on the most abundant ion in those full scans. The first automatically acquired a high-resolution (zoom) scan for determination of the charge state; the second (MS/MS) scan gathered the peptide sequence information. The MS/MS spectra were acquired with a relative collision energy of 35 and an isolation width of 2.5 Da. Interpretation of the resulting MS/MS spectra was facilitated by database correlation with the algorithm SEQUEST.[10]

Reverse transcription (RT), polymerase chain reaction (PCR) and DNA sequencing

We performed RT-PCR to obtain the deduced amino acid sequence of porcine MLC-2V. The primer pair was designed according to the consensus sequence of human, canine and rat MLC-2V. The forward primer was 5'-GAGGCAGTGCTGGGTCCTTT and the reverse primer was 5'-CCACCCAGGCTGCAAAGAAG. The reaction was carried out with a denaturing temperature of 95^{o}C, annealing temperature of 55^{o}C and extension temperature of 72^{o}C for 35 cycles. The size of the product was confirmed by agarose gel electrophoresis and DNA sequencing reaction was performed using Big Dye Terminator chemistry on a 377 ABI PRISM DNA sequencer (Perkin-Elmer, Wellesley, MA, USA).

Quantitative real time RT-PCR

Quantitative real-time RT-PCR was used to measure the relative mRNA amount of MLC-2V in porcine and human left atrial samples. Triplicate aliquots of each RNA sample were used in the reactions. Glyceraldehyde-3-phosphate dehydrogenase (GAPDH) was used as the internal control. One-step real-time RT-PCR was performed using TaqMan PCR Master Mix reagent kit (Perkin-Elmer Applied Biosystems, Foster City, CA). All reactions were carried out in 50-µl volumes containing 0.5 µl of RNaseOUT RNase inhibitor, 50 ng of sample RNA, each forward and reverse primer in 300nM and fluorescently labeled probes in 250nM (Table 1). Reactions were performed in the Perkin-Elmer ABI Prism 7700 sequence detection system. We recorded the threshold cycle value (C_T), which represents the cycle at which a statistically significant increase in the normalized reporter signal above a chosen threshold can first be detected, according to the manufacturer's manual. The $\Delta\Delta C_T$ method was used to quantify the MLC2V mRNA and GAPDH.[11] A relative expression value of MLC2V to GAPDH was obtained. Fold differences were calculated by dividing the mean of Af samples by the normal samples.

Statistical analyses

For cDNA microarray experiments, a foreground over background ratio of more than 1.5 was considered a significant expression[12] and genes without significant expression in both Af and control groups were excluded from analysis. The gene

expression intensities were represented by foreground intensities subtracting background intensities. The intensities were further normalized to the mean intensity of all genes on the same slide. Differential expression values were calculated as the ratio of Cy5 to Cy3 intensities (Af to control). One sample *t* test was used to calculate the p value of whether the ratio was different from the unit. A significant increase or decrease of gene expression was defined as a ratio >2.5 or < 0.4 (2.5 fold increase or decrease) together with a p value < 0.05.[12]

To examine if the Af tissue had a distinct gene expression pattern, hierarchical analysis was performed using the Cluster and Treeview program by Eisen et al.[13]

Parametric data were compared between the Af and control groups using Student's *t* test. A p value < 0.05 was considered statistically significant.

Results

Of the twelve pigs, 6 pigs with active pacing for 4 weeks all showed Af at the end of pacing. The Af persisted after turning off the pacemaker for 2 weeks until they were sacrificed. For the other 6 pigs with shamed-operation, sinus rhythm was observed 4 weeks after the operation. These pigs had sinus rhythm through out the study period.

Differences in gene expression in Af

Among the 6053 genes, 387 genes showed a significant change of expression level in the left atrium. Among these, 102 genes showed a fold of change greater than

2.5 (Cy5/Cy3 >2.5) and 285 showed a fold of change less than 0.4 (Cy3/Cy5>2.5). In the right atrium, there were 81 genes showing a significant change, with 40 showing a significant increase and 41 showing a significant decrease. Among the 81 genes showing a significant change in the right atrium, 39 genes also showed a significant change concordantly in the left atrium (Table 2). Table 3 and 4 show the 10 most significantly upregulated and downregulated genes in the left and right atria respectively. Since there were more genes showing significant change in the left atrium, we performed clustering analysis for the gene expression changes in the left atrium. Figure 1 shows the dendrogram of the results of hierarchical analysis in the left atrium. The brightness of the bars in the figure denotes the level of expression. Through the visual display in Figure 1, it is evident that the expression patterns were similar for pigs in the same group (Af group or control group) and the Af tissue had distinct gene expression patterns from control tissues.

Expression patterns in functional categories

Genes were classified into 7 functional categories according to the biological function of the encoded protein using a previously established classification scheme.[14] Figure 2 shows the number of significantly changed genes by different functional categories. The genes involved in cell signaling/communication outnumbered the genes in other category. Genes involved in transcription/translation regulation had the second largest number of genes. Table 5 and 6 list the genes with significant change in the left atrium in both categories respectively.

2D-PAGE and MS analysis

Figure 3 shows representative results of the 2D-PAGE. The protein pattern was consistent in all twelve gels and the pattern was also similar to previous published human atrial tissue 2D-PAGE images. With regard to the changes in the gels, an obvious change could be detected by visual inspection, as indicated by arrows in Figure 3. These protein spots were at PI 4.5 to 5.0 with molecular weights about 18 to 20 kD. The total optical density number of the three protein spots was significantly higher in the Af group than in the control group (1.35±0.53 vs 0.39±0.52, in arbitrary unit, $p < 0.01$). To identify the nature of the three protein spots, these protein spots were cut from the gel and subjected to mass spectrometry analysis. The amino acid sequences of four peptide fragments were obtained. A BLASTp search result showed that all the four fragments matched with the ventricular isoform of myosin regulatory light chain (MLC-2V) (Fig. 4). Therefore, the three spots were all MCL-2V probably with different degrees of phosphorylation.

Because the ventricular isoform of the MLC-2 was significantly increased in pigs with Af, we also calculated the MLC-2V/MLC-2A ratio using total optical density number of both proteins in the 2D-PAGE. We found that the ratio was significantly increased in the Af group (0.85±0.54 vs 0.16±0.17, $p<0.014$).

RT-PCR and DNA sequencing

Agarose gel electrophoresis of the RT-PCR products for MLC-2V showed a single band with a predicted size. Further DNA sequencing reaction was performed

and the base sequence of the coding region of MLC-2V was obtained. The sequence was deposited in GenBank with an accession number of AF513016. When translated to protein, the deduced amino acid sequence was 97% homologous to canine MLC-2V, 96% to human MLC-2V, 95% to rat MLC-2V and 93% to mouse MLC-2V. Figure 4 shows the alignment of the MLC-2V amino acid sequence among different species with the 4 peptidal fragments identified by MS in rectangles.

Quantitative real time RT-PCR

Quantitative real time RT-PCR was performed to confirm the change of MLC-2V mRNA in porcine tissue. The fold of change was 8.72 ($p< 0.036$), which was very similar to that detected in microarray studies (9.24, $p <0.016$).

.

Discussion

Recent bio-technological advances in DNA microarray and 2D-PAGE have made it possible to investigate the changes of mRNAs and proteins of thousands of genes simultaneously. In the present study, we successfully applied these techniques to profile the changes in Af tissue. We showed that Af tissue had distinct gene expression patterns after 6 weeks of rapid atrial depolarization. We also identified MLC-2V as the most significantly changed gene at both mRNA and protein levels. The changes of MLC-2V mRNA were further confirmed by quantitative real time RT-PCR in porcine and human left atrial tissues. To the best of our knowledge, this is the first report to screen the alterations in Af tissue in genomic and proteomic views.

In the cDNA microarray study, we found that the changes in the left atrium were more prominent than those in the right atrium, though there was considerable overlap. The reason why the left atrium had more significantly changed genes was not clear. However, we propose some possible mechanisms. First, it has been reported that the left atrium has a shorter cycle length than the right atrium during Af. This means that the left atrium was excited at an even faster rate than the right atrium during Af. Second, Af with rapid ventricular rate might induce heart failure and increased left ventricular end diastolic pressure. This pressure might cause increased left atrial stretch and contribute to more gene expression changes.

Comparison with other studies on changes in Af

The present study has several unique features when compared with previous studies. First, thousands of genes were screened simultaneously. Previous studies focused on only a limited number of genes with a candidate gene approach. With such an approach, only genes involving known related pathways were chosen. Furthermore, we investigated the changes in Af tissue at a relatively early stage of Af (6 weeks) as compared to many clinical studies. Clinical investigations are usually performed at a late stage of disease because atrial tissues are usually obtained during open heart surgery when the patients have medical refractory conditions. However, Af was induced by rapid atrial pacing in the present study. It is possible that the pathophysiological pathways are different from clinical Af, which is commonly caused by heart failure, hypertension, valvular lesions, atrial stretch and so on.[15]

There are many past studies that focus on the changes in ion channels because Af is a disease of electric impulse generation and propagation. Among the studies on ion channels, downregulation of L-type calcium channel is the most reproducibly reported one. It is directly linked to the shortening of the atrial effective refractory period and plays important roles in the perpetuation of Af. In comparison to these studies, we also found that the mRNA of the pore-forming subunit (α_{1C} subunit) of the L-type calcium channel was significantly reduced in the left atrium (fold of change = 0.37, $p < 0.05$) and borderlinely reduced in the right atrium (fold of change = 0.51, not < 0.4 but $p < 0.05$). This finding is consistent with those in previous studies.[3,16,17] In addition, we further identified a substantial number of altered genes regarding cell signaling/communication and transcription/translation regulation (protein/gene expression). The findings might suggest that changes in regulatory genes occur relatively early in Af and these changes have rarely been reported before. The changes in cell signaling/communication and transcription/translation regulation in Af may be fundamental and deserve future investigations.

Myosin light chain 2-V

Microarray studies identified MLC-2V as the most significantly upregulated gene. However, identifying MLC-2V as the increased protein was not straightforward. We first identified three protein spots with a significant increase in 2D-PAGE. However, further analysis was hampered because the data bank of porcine proteins is very limited. With the aid of tandem chromatography MS, we finally identified

MLC-2V as the protein spots. We further used molecular cloning techniques to solve the porcine MLC-2V cDNA coding sequences and protein sequences.

MLC-2 is also named as the regulatory light chain because phosphorylation of this protein modifies force development muscle. In cardiac myocyte shortening, it has been demonstrated that cardiac MLC-2 phosphorylation produces a dramatic increase in the sensitivity of tension development to increasing extra-cellular calcium concentrations.[18] MLC-2 proteins are encoded by a multiple gene family, giving rise to a number of isoforms that are expressed in a tissue specific manner. In adult atrial tissue, the MLC-2A is the atrial isoform while the ventricle contains the ventricular isoform (MLC-2V). In the present study, we demonstrated an alteration of the MLC-2 isoform composition in fibrillating atrial tissue. There was a dramatic increase of the MLC-2V mRNA in the atrial tissue (9.42 and 7.27 fold increase in LA and RA respectively) while the MLC-2A mRNA was only mildly elevated (2.61 and 2.56 fold increase in LA and RA respectively). As to the protein level, the MLC-2V protein amount increased significantly while MLC-2A showed no significant change (Fig 3). This resulted in a much higher MCL-2V/MLC-2A ratio. Since MLC-2 is an important regulator of muscle contraction, the alteration in isoform composition should have important functional implication in Af. In a report on experiments on transgenic mice, the total replacement of MLC-2A with MLC-2V resulted in an enhanced contractility and decreased amplitude of calcium transient in atrial myocytes.[19,20] The cross bridge cycling rate was faster in the presence of MLC-2V. Such kind of alteration in MLC-2

composition has also been reported in spontaneous hypertensive rats as well as in human right atria from patients with various kinds of heart disease.[21,22] With the reprogramming of MLC-2 isoform expression in Af, we expect changes in contractile force and cross bridge cycling properties, which might be important in the pathogenesis of Af. However, with only limited studies in small animals with this regard, the functional consequence and clinical significance of this alteration in Af deserve further investigation.

Limitations

We used human cDNA microarrays to profile the gene expression pattern in porcine myocardial tissue. Although interspecies cross reactivity has been reported,[23] as yet there were no specific data available regarding human and porcine cross reactivity. In microarray studies using cDNA clones greater than 100 base pairs (not oligonucleotides), the binding of probes and clones are similar to Southern and Northern blotting techniques, in which interspecies cross reactivity is well known.

Pulmonary venous tissue is important in the initiation or maintenance of atrial fibrillation.[24] Unfortunately, the tissue sample collected did not include pulmonary venous tissue. We believe that future research to profile the pulmonary venous tissue gene expression pattern will be very important.

Functional studies regarding the consequences of myosin regulatory light chain isoform reprogramming were not performed in the present study. The cDNA microarray used in the present study contained known genes only. This had the

advantage of ready to go sequence information for further study. However, novel genes with significant changes could not be found. The cDNA microarray and 2D-PAGE techniques are high through-put screening methods. These screening investigations provide a list of potentially important genes and protein spots. For the genes or spots identified with significant changes, further investigations are needed to confirm the changes as well as to explore the functional and therapeutic importance of the changes. Expression information itself is not sufficient to establish a pathophysiological pathway critical to Af. However, the database provided here is very useful in generating a testable hypothesis.

The data in the present manuscript represent changes observed after 6 weeks of rapid atrial depolarization. A time course information is not provided. It is possible that a transient change at an earlier stage may have been missed in the present study.

Acknowledgement

We appreciate excellent technical help from Ms. Lilian Chung and Ms. Mu-Ying Kuo. The GAPDH probe for quatitative real time RT-PCR was a generous gift from PE-ABI, Taiwan.

References

1. Wijffels MC, Kirchhof CJ, Dorland R, Power J, Allessie MA.. Atrial fibrillation begets atrial fibrillation. A study in awake chronically instrumented goats. Circulation 1995;92:1954-68.

2. Lai LP, Su MJ, Lin JL, Tsai CH, Lin FY, Chen YS, Hwang JJ, Huang SKS, Tseng YZ, Lien WP. Measurement of funny current (I_f) channel mRNA in human atrial tissue: correlation with left atrial filling pressure and atrial fibrillation. J Cardiovasc Electrophysiol 1999;10:947-53.

3. Lai LP, Su MJ, Lin JL, Lin FY, Tsai CH, Chen YS, Huang SKS, Tseng YZ, Lien WP. Down-regulation of L-type calcium channel and sarcoplasmic reticular Ca(2+)-ATPase mRNA in human atrial fibrillation without significant change in the mRNA of ryanodine receptor, calsequestrin and phospholamban: an insight into the mechanism of atrial electrical remodeling. J Am Coll Cardiol 1999;33:1231-7.

4. Goette A, Arndt M, Rocken C, Spiess A, Staack T, Geller JC, Huth C, Ansorge S, Klein HU, Lendeckel U. Regulation of angiotensin II receptor subtypes during atrial fibrillation in humans. Circulation 2000;101:2678-81.

5. Grammer JB, Zeng X, Bosch RF, Kuhlkamp V. Atrial L-type Ca2+-channel, beta-adrenoreceptor, and 5-hydroxytryptamine type 4 receptor mRNAs in human atrial fibrillation. Basic Res Cardiol 2001;96:82-90.

6. Duggan DJ, Bittner M, Chen Y, Meltzer P, Trent JM. Expression profiling using cDNA microarrays. Nat Genet 1999;21:10-4.

7. Klose J, Kobalz U. Two-dimensional electrophoresis of proteins: an updated protocol and implications for a functional analysis of the genome. Electrophoresis 1995;16:1034-59.

8. Lin JL, Lai LP, Lin CS, Du CC, Wu TJ, Chen SP, Lee WC, Yang PC, Tseng YZ, Lien WP, Huang SKS. Electrophysiological mapping and histological examinations of the swine atrium with sustained (≧24 h) atrial fibrillation: a suitable animal model for studying atrial fibrillation. Cardiology 2003;99:78-84.

9. Tsay YG, Wang YH, Chiu CM, Shen BJ, Lee SC. A strategy for identification and quantitation of phosphopeptides by liquid chromatography/tandem mass spectrometry. Anal Biochem 2000;287:55-64.

10. Eng JK, McCormick AL, Yates JR. An approach to correlate tandem mass spectral data of pep-tides with amino acid sequences in a protein database. J Am Soc Mass Spectrom 1994;5:976-89.

11. Winer J, Jung CK, Shackel I, Williams PM. Development and validation of real-time quantitative reverse transcriptase-polymerase chain reaction for monitoring gene expression in Cardiac myocytes in vitro. Analytical Biochemistry 1999;270:41-9.

12. Hwang JJ, Allen PD, Tseng GC, Lam CW, Fananapazir L, Dzau VJ, Liew CC. Microarray gene expression profiles in dilated and hypertrophic cardiomyopathic end-stage heart failure. Physiol Genomics 2002;10:31-44.

13. Eisen MB, Spellman PT, Brown PO, Botstein D. Cluster Analysis and Display of Genome-Wide Expression Patterns. Proc Natl Acad Sci 1998;95:14863-8.

14. Adams MD, Kerlavage AR, Fleischmann RD, Fuldner RA, Bult CJ, Lee NH, Kirkness EF, Weinstock KG, Gocayne JD, White O, Sutton G, Blake JA, Brandon RG, Chiu MW, Clayton RA, Cline RTt, Cotton MDd, Earlehughes J, Fine LDd, Fitzgerald LMm, Fitzhugh WM, Fritchman JLl, Geoghagen NSM, Glodek A, Gnehm CL, Hanna MC, Hedblom E, Hinkle PS, Kelley JM, Klimek KM, Kelley JC, Liu LI, Marmaros SM, Merrick JM, Morenopalanques RF, Mcdonald LA, Nguyen DT, Pellegrino SM, Phillips CA, Ryder SE, Scott JL, Saudek DM, Shirley R, Small KV, Spriggs TA, Utterback TR, Weldman JF, Li Y, Barthlow R, Bednarik DP, Cao LA, Cepeda MA, Coleman TA, Collins EJ, Dimke D, Feng P, Ferrie A, Fischer C, Hastings GA, He WW, Hu JS, Huddleston KA, Greene JM, Gruber J, Hudson P, Kim A, Kozak DL, Kunsch C, Ji HJ, Li HD, Meissner PS, Olsen H, Raymond L, Wei YF, Wing J, Xu C, Yu GL, Ruben SM, Dillon PJ, Fannon MR, Rosen CA, Haseltine WA, Fields C, Fraser CM, Venter JC. Initial assessment of human gene diversity and expression patterns based upon 83 million nucleotides of cDNA sequence. Nature 1995;377(suppl):3-174.

15. Allessie M, Ausma J, Schotten U. Electrical, contractile and structural

remodeling during atrial fibrillation. Cardiovasc Res. 2002;54:230-46.

16. Van Gelder IC, Brundel BJ, Henning RH, Tuinenburg AE, Tieleman RG, Deelman L, Grandjean JG, De Kam PJ, Van Gilst WH, Crijns HJ. Alteration in gene expression of proteins involved in the calcium handling in patients with atrial fibrillation. J Cardiovasc Electrophysiol 1999;10:552-60.
17. Brundel BJ, van Gelder IC, Henning RH, Tuinenburg AE, Deelman LE, Tieleman RG, Grandjean JG, van Gilst WH, Crijns HJ. Gene expression of proteins influencing the calcium homeostasis in patients with persistent and paroxysmal atrial fibrillation. Cardiovasc Res 1999;42:443-54.
18. Moore RL, Musch TI, Cheung JY. Modulation of cardiac contractility by myosin light chain phosphorylation. Med Sci Sports Exerc 1991;23:1163-9.
19. Buck SH, Konyn PJ, Palermo J, Robbins J, Moss RL. Altered kinetics of contraction of mouse atrial myocytes expressing ventricular myosin regulatory light chain. Am J Physiol 1999;276:H1167-71.
20. Pawloski-Dahm CM, Song G, Kirkpatrick DL, Palermo J, Gulick J, Dorn GW, Robbins J, Walsh RA. Effects of total replacement of atrial myosin light chain-2 with the ventricular isoform in atrial myocytes of transgenic mice. Circulation 1998;97:1508-13.
21. Kumar C, Saidapet C, Delaney P, Mendola C, Siddiqui MA. Expression of ventricular-type myosin light chain messenger RNA in spontaneously hypertensive rat atria. Circ Res 1988;62:1093-7.

22. Wankerl M, Bohm M, Morano I, Ruegg JC, Eichhorn M, Erdmann E. Calcium sensitivity and myosin light chain pattern of atrial and ventricular skinned cardiac fibers from patients with various kinds of cardiac disease. J Mol Cell Cardiol 1990;22:1425-38.

23. Dong Y, Glasner JD, Blattner FR, Triplett EW. Genomic interspecies microarray hybridization: rapid discovery of three thousand genes in the maize endophyte, Klebsiella pneumoniae 342, by microarray hybridization with Escherichia coli K-12 open reading frames. Appl Environ Microbiol 2001;67:1911-21.

24. Haissaguerre M, Jais P, Shah DC, Takahashi A, Hocini M, Quiniou G, Garrigue S, Le Mouroux A, Le Metayer P, Clementy J. Spontaneous initiation of atrial fibrillation by ectopic beats originating in the pulmonary veins. N Engl J Med 1998;339:659-66.

Legend to Figure

Figure 1: Dendrogram showing the gene expression patterns in the left atrial tissue from 6 pigs with atrial fibrillation and 6 control pigs. The expression level is represented by the brightness of the bars. Pigs with the most similar expression patterns were linked by lines and positioned side by side. Relatedness was calculated again for the next most similar expression patterns and the process was repeated until all the pigs were positioned in the dendrogram. Through this visual display, it is evident that the 6 pigs with atrial fibrillation had distinct gene expression pattern from the 6 control pigs. AF = atrial fibrillation, SR = sinus rhythm.

Figure 2: The number of significantly changed genes by different functional categories. The genes involved in cell signaling/communication outnumbered the genes in other categories. Genes involved in protein/gene expression had the second largest number of genes.

Figure 3: Representative two-dimensional protein electrophoresis results by silver stain. The two gels have similar patterns. The major differences are the three protein spots (indicated by arrow heads) at PI 4.5 to 5.0 with molecular weight of 18 to 20 kD, which can be easily identified by visual inspection.

Figure 4: Amino acid sequence of the porcine myosin regulatory light chain ventricular isoform deduced from the sequencing results in RT-PCR product. The regions in rectangulars represent the fragments identified by mass spectrometry. The sequences of dog, human, rat and mouse were listed for comparison.

Table 1. Base sequences of the primers and probes used for quantitative real-time reverse transcription-polymerase chain reaction

	Sequence
MLC2V	
Forward primer	AGGTGTCCCTCAGATCATTCTTG
Reverse primer	CAGGAATTTAAGGAGGCCTTCA
Probe (5'labeled-Fam)	AAGCCATCCCTGTTCTGGTCCATGATG
GAPDH	
Forward primer	CAGCAATGCCTCCTGTACCA
Reverse primer	GATGCCGAAGTTGTCATGGA
Probe (5'labeled-Vic)	AACTGCTTGGCACCCCTGGCC

Table 2: Genes showing significant change in both left and right atrium

Name of gene	left atrium		right atrium	
	FOC	p	FOC	p
myosin, light polypeptide 2, regulatory, cardiac, slow	9.42	0.016	7.27	0.038
ribosomal protein L35	5.21	0.017	4.13	0.021
crystallin, alpha B	4.83	0.010	2.68	0.003
cysteine and glycine-rich protein 3 (cardiac LIM protein)	4.29	0.032	2.62	0.002
collagen, type VI, alpha 2	4.27	0.007	2.51	0.002
Human cytoplasmic beta-actin gene	4.21	0.029	2.74	0.000
adenine nucleotide translocator 1 (skeletal muscle)	3.92	0.011	3.90	0.017
actin, gamma 2, smooth muscle, enteric	3.84	0.046	2.74	0.014
Human mRNA for calmodulin	3.80	0.017	3.18	0.000
fatty acid binding protein 3, muscle and heart	3.62	0.013	3.23	0.004
phosphodiesterase 6A, cGMP-specific, rod, alpha	3.57	0.005	2.84	0.001
phosphate carrier, mitochondrial	3.53	0.024	2.85	0.014
adenosine A2a receptor	3.49	0.036	2.88	0.008
ras-related C3 botulinum toxin substrate 1	3.44	0.008	2.60	0.000
ATP synthase, H+ transporting, mitochondrial F1 complex, beta polypeptide	3.37	0.010	3.56	0.030
amyloid beta (A4) precursor protein	3.36	0.014	2.51	0.001
voltage-dependent anion channel 2	3.11	0.028	2.56	0.002
ATP synthase, H+ transporting, mitochondrial F0 complex, subunit c (subunit 9) isoform 3	3.00	0.018	2.84	0.032
clathrin, light polypeptide (Lcb)	2.97	0.011	2.71	0.012
Human acidic ribosomal phosphoprotein P0	2.95	0.003	2.86	0.001
phosphofructokinase, muscle	2.93	0.011	2.74	0.009
peptidylglycine alpha-amidating monooxygenase	2.91	0.018	3.06	0.017
citrate synthase	2.86	0.000	2.50	0.009
Tubulin, alpha, brain-specific	2.86	0.004	2.52	0.000
patched (Drosophila) homolog	2.68	0.017	2.52	0.004
HUMMLC2At; Homo sapiens; ; 593 base-pairs	2.62	0.035	2.57	0.039
homeo box D3	2.60	0.023	2.56	0.018
ubiquitin A-52 residue ribosomal protein fusion product 1	2.60	0.005	2.53	0.000
B-cell CLL/lymphoma 3	0.39	0.000	0.38	0.003
neurotrophic tyrosine kinase, receptor-related 2	0.37	0.000	0.34	0.000
wingless-type MMTV integration site family member 2	0.37	0.000	0.40	0.000

meningioma expressed antigen 6	0.36	0.000	0.38	0.000
carnitine palmitoyltransferase II	0.35	0.000	0.40	0.000
pleiomorphic adenoma gene 1	0.35	0.000	0.36	0.000
selectin L (lymphocyte adhesion molecule 1)	0.35	0.000	0.36	0.000
guanylate binding protein 2	0.35	0.000	0.38	0.000
caspase 1, apoptosis-related cysteine protease	0.33	0.000	0.33	0.000
Human translation initiation factor eIF-2alpha	0.32	0.000	0.37	0.000
guanylate cyclase 1, soluble, beta 3	0.29	0.000	0.38	0.001

FOC = fold of change.

Table 3: The ten most up- and down-regulated genes in the left atrium

Name of Gene	UniGene	FOC	p
Myosin, light polypeptide 2, regulatory, cardiac, slow	Hs.75535	9.42	0.016
ribosomal protein L35	Hs.182825	5.21	0.017
crystallin, alpha B	Hs.1940	4.83	0.010
secreted protein, acidic, cysteine-rich (osteonectin)	Hs.111779	4.59	0.001
protein tyrosine phosphatase, receptor type, c polypeptide	Hs.170121	4.29	0.002
cysteine and glycine-rich protein 3 (cardiac LIM protein)	Hs.83577	4.29	0.032
collagen, type VI, alpha 2	Hs.4217	4.27	0.007
Human cytoplasmic beta-actin gene	Hs.288061	4.21	0.029
four and a half LIM domains 1	Hs.239069	4.20	0.005
Adenine nucleotide translocator 1 (skeletal muscle)	Hs.2043	3.92	0.011
cathepsin S	Hs.181301	0.17	0.000
chromosome 8 open reading frame 1	Hs.40539	0.15	0.000
leukemia associated gene 2	Hs.43628	0.14	0.000
glycogenin 2	Hs.58589	0.14	0.000
PTD010 protein	Hs.182470	0.13	0.000
Fas (TNFRSF6)-associated via death domain	Hs.86131	0.13	0.000
Claudin 1	Hs.7327	0.10	0.000
sperm associated antigen 6	Hs.158213	0.10	0.000
prostaglandin E receptor 3 (subtype EP3)	Hs.170917	0.09	0.000
DEAD/H (Asp-Glu-Ala-Asp/His) box polypeptide 9 (RNA helicase A, nuclear DNA helicase II; leukophysin)	Hs.74578	0.03	0.002

FOC = fold of change; UniGene = accession number in UniGene data bank.

Table 4: The ten most up- and down-regulated genes in the right atrium

Name of Gene	UniGene	FOC	p
Myosin, light polypeptide 2, regulatory, cardiac, slow	Hs.75535	7.27	0.038
ribosomal protein L35	Hs.182825	4.13	0.021
Human mitochondrial ADP/ADT translocator mRNA	Hs.2043	3.94	0.011
ATP synthase, H+ transporting, mitochondrial F1 complex, beta polypeptide	Hs.25	3.56	0.030
fatty acid binding protein 3, muscle and heart (mammary-derived growth inhibitor)	Hs.49881	3.23	0.004
Human mRNA for calmodulin	Hs.182278	3.18	0.000
Spermidine/spermine N1-acetyltransferase mRNA	Hs.28491	3.14	0.004
peptidylglycine alpha-amidating monooxygenase	Hs.83920	3.06	0.017
Nucleolin	Hs.79110	2.95	0.028
adenosine A2a receptor	Hs.1613	2.88	0.008
tissue factor pathway inhibitor (lipoprotein-associated coagulation inhibitor)	Hs.170279	0.36	0.001
v-akt murine thymoma viral oncogene homolog 2	Hs.200816	0.36	0.000
pleiomorphic adenoma gene 1	Hs.14968	0.36	0.000
p21 (CDKN1A)-activated kinase 3	Hs.152663	0.35	0.000
Inositol 1,4,5-trisphosphate 3-kinase B	Hs.78877	0.34	0.000
neurotrophic tyrosine kinase, receptor-related 2	Hs.155585	0.34	0.000
caspase 1, apoptosis-related cysteine protease (interleukin 1, beta, convertase)	Hs.2490	0.33	0.000
arginine vasopressin receptor 1A	Hs.2131	0.32	0.000
solute carrier family 7 (cationic amino acid transporter, y+ system), member 6	Hs.10315	0.31	0.001
hydroxy-delta-5-steroid dehydrogenase, 3 beta- and steroid	Hs.38586	0.28	0.000

delta-isomerase 1

FOC = fold of change; UniGene = accession number in UniGene data bank.

Table 5: Genes in the cell signaling/communication category showing significant changes in the left atrium

Name of Gene	UniGene	FOC	p
crystallin, alpha B	Hs.1940	4.83	0.010
apolipoprotein D	Hs.75736	3.91	0.007
Human mRNA for calmodulin	Hs.182278	3.80	0.017
thymosin, beta 4, X chromosome	Hs.75968	3.80	0.016
S100 calcium-binding protein A1	Hs.255978	3.78	0.001
annexin A4	Hs.77840	3.67	0.014
adenosine A2a receptor	Hs.1613	3.49	0.036
ras-related C3 botulinum toxin substrate 1 (rho family, small GTP binding protein Rac1)	Hs.173737	3.44	0.008
Human aminoacylase-1 (ACY1)	Hs.334707	3.13	0.042
nuclear receptor subfamily 4, group A, member 1	Hs.1119	3.12	0.003
voltage-dependent anion channel 2	Hs.78902	3.11	0.028
connective tissue growth factor	Hs.75511	3.03	0.040
ATP synthase, H+ transporting, mitochondrial F0 complex, subunit c (subunit 9) isoform 3	Hs.429	3.00	0.018
Human malate dehydrogenase (MDHA)	Hs.75375	2.92	0.031
H.sapiens mRNA for elongation factor-1-gamma	Hs.256184	2.90	0.016
Human guanine nucleotide-binding protein G-s, alpha subunit	Hs.374523	2.81	0.026
creatine kinase, mitochondrial 2 (sarcomeric)	Hs.80691	2.65	0.012
heterogeneous nuclear ribonucleoprotein A2/B1	Hs.75598	2.62	0.028
peroxisome proliferative activated receptor, delta	Hs.106415	2.61	0.002
protease inhibitor 6 (placental thrombin inhibitor)	Hs.41072	2.56	0.013
thymosin, beta 10	Hs.76293	2.55	0.013
thrombospondin 4	Hs.75774	2.54	0.013
phospholemman	Hs.160318	2.51	0.000
CDC28 protein kinase 2	Hs.83758	0.40	0.000
insulin-like growth factor binding protein 3	Hs.77326	0.40	0.000
3-hydroxyisobutyryl-Coenzyme A hydrolase	Hs.236642	0.40	0.000
frizzled (Drosophila) homolog 7	Hs.173859	0.40	0.000
nucleoporin 62kD	Hs.247460	0.39	0.000
fibulin 2	Hs.198862	0.39	0.000
guanine nucleotide binding protein (G protein), beta polypeptide 1	Hs.76064	0.39	0.000
B-cell CLL/lymphoma 3	Hs.31210	0.39	0.000
doublecortin and CaM kinase-like 1	Hs.21355	0.39	0.000
branched chain keto acid dehydrogenase E1, beta polypeptide (maple syrup urine disease)	Hs.1265	0.39	0.000

tumor necrosis factor (ligand) superfamily, member 10	Hs.83429	0.38	0.000
golgi SNAP receptor complex member 2	Hs.100651	0.38	0.000
NIMA (never in mitosis gene a)-related kinase 2	Hs.153704	0.38	0.000
tumor necrosis factor receptor superfamily, member 10b	Hs.258205	0.38	0.000
catenin (cadherin-associated protein), alpha-like 1	Hs.58488	0.38	0.000
neurotrophic tyrosine kinase, receptor-related 2	Hs.155585	0.37	0.000
calcium channel, voltage-dependent, L type, alpha 1C subunit	Hs.260083	0.37	0.000
PAK-interacting exchange factor beta	Hs.172813	0.37	0.000
SEC22, vesicle trafficking protein (S. cerevisiae)-like 1	Hs.50785	0.37	0.000
Phosphatidic acid phosphatase type 2a	Hs.41569	0.36	0.000
spondin 1, (f-spondin) extracellular matrix protein	Hs.5378	0.36	0.000
solute carrier family 11 (proton-coupled divalent metal ion transporters), member 2	Hs.261269	0.36	0.000
phosphoinositide-3-kinase, catalytic, gamma polypeptide	Hs.32942	0.36	0.000
granzyme K (serine protease, granzyme 3; tryptase II)	Hs.3066	0.36	0.000
leukemia inhibitory factor receptor	Hs.2798	0.36	0.000
diacylglycerol kinase, delta (130kD)	Hs.241489	0.35	0.000
3-hydroxyisobutyryl-Coenzyme A hydrolase	Hs.236642	0.35	0.000
a disintegrin and metalloproteinase domain 12 (meltrin alpha)	Hs.266112	0.35	0.000
vaccinia related kinase 2	Hs.82771	0.35	0.000
thyroid hormone receptor interactor 6	Hs.119498	0.35	0.000
nuclear matrix protein p84	Hs.1540	0.35	0.000
Homo sapiens cytokine receptor related protein 4 (CYTOR4)	Hs.259518	0.35	0.000
interferon, alpha-inducible protein (clone IFI-6-16)	Hs.251988	0.35	0.000
guanylate cyclase 1, soluble, alpha 3	Hs.75295	0.35	0.000
selectin L (lymphocyte adhesion molecule 1)	Hs.82848	0.35	0.000
guanine nucleotide binding protein (G protein), alpha activating activity polypeptide, olfactory type	Hs.154145	0.35	0.000
dual-specificity tyrosine-(Y)-phosphorylation regulated kinase 2	Hs.250573	0.35	0.000
guanylate binding protein 2, interferon-inducible	Hs.171862	0.35	0.000
pericentriolar material 1	Hs.75737	0.35	0.000
growth factor receptor-bound protein 14	Hs.83070	0.35	0.000
solute carrier family 6 (neurotransmitter transporter, GABA), member 1	Hs.22003	0.35	0.000
nuclear receptor coactivator 2	Hs.256646	0.34	0.002
FK506-binding protein 5	Hs.7557	0.34	0.000
solute carrier family 5 (inositol transporters), member 3	Hs.253283	0.33	0.000
Homo sapiens Williams-Beuren syndrome chromosome	Hs.21075	0.33	0.000

region 11 (WBSCR11) mRNA			
transferrin receptor (p90, CD71)	Hs.77356	0.33	0.000
polymerase (DNA-directed), alpha (70kD)	Hs.81942	0.32	0.000
SRY (sex-determining region Y)-box 9 (campomelic dysplasia, autosomal sex-reversal)	Hs.2316	0.32	0.000
Homo sapiens genes encoding RNCC protein, DDAH protein, Ly6-C protein, Ly6-D protein and immunoglobulin receptor	Hs.241586	0.31	0.000
GM2 ganglioside activator protein	Hs.169476	0.31	0.000
solute carrier family 12 (sodium/potassium/chloride transporters), member 2	Hs.110736	0.31	0.000
protein phosphatase, EF hand calcium-binding domain 1	Hs.254709	0.31	0.000
frizzled (Drosophila) homolog 1	Hs.94234	0.31	0.000
integrin, alpha 2 (CD49B, alpha 2 subunit of VLA-2 receptor)	Hs.1142	0.30	0.000
retinoblastoma-binding protein 1	Hs.91797	0.30	0.000
grancalcin	Hs.79381	0.30	0.000
solute carrier family 26 (sulfate transporter), member 2	Hs.29981	0.30	0.000
aquaporin 4	Hs.252151	0.29	0.000
RAS p21 protein activator (GTPase activating protein) 1	Hs.758	0.29	0.000
guanylate cyclase 1, soluble, beta 3	Hs.77890	0.29	0.000
thymopoietin	Hs.250957	0.29	0.000
phosphorylase kinase, beta	Hs.78060	0.29	0.000
transferrin receptor (p90, CD71)	Hs.77356	0.28	0.000
natural killer cell receptor, immunoglobulin superfamily member	Hs.81743	0.28	0.000
serine/threonine kinase 17a (apoptosis-inducing)	Hs.9075	0.27	0.000
hyaluronan-mediated motility receptor (RHAMM)	Hs.258169	0.27	0.000
synaptosomal-associated protein, 23kD	Hs.184376	0.27	0.000
protein phosphatase 2 (formerly 2A), regulatory subunit A (PR 65), beta isoform	Hs.108705	0.27	0.000
ras GTPase activating protein-like	Hs.227806	0.26	0.000
gamma-aminobutyric acid (GABA) A receptor, alpha 2	Hs.91343	0.26	0.000
guanylate cyclase 1, soluble, alpha 3	Hs.75295	0.25	0.000
rab3 GTPase-activating protein, non-catalytic subunit (150kD)	Hs.197289	0.25	0.000
eukaryotic translation elongation factor 1 epsilon 1	Hs.172247	0.21	0.000
5-hydroxytryptamine (serotonin) receptor 2A	Hs.256867	0.18	0.000
solute carrier family 5 (inositol transporters), member 3	Hs.172455	0.17	0.000
claudin 1	Hs.7327	0.10	0.000
prostaglandin E receptor 3 (subtype EP3)	Hs.170917	0.09	0.000

FOC = fold of change; UniGene = accession number in UniGene data bank.

Table 6: Genes in the protein/gene expression category showing significant changes in the left atrium

Name of Gene	UniGene	FOC	p
ribosomal protein L35	Hs.182825	5.21	0.017
Human mitochondrial ADP/ADT translocator	Hs.2043	3.67	0.014
phosphodiesterase 6A, cGMP-specific, rod, alpha	Hs.182240	3.57	0.005
interleukin 10 receptor, beta	Hs.173936	3.37	0.006
fatty acid binding protein 3, muscle and heart (mammary-derived growth inhibitor)	Hs.49881	3.21	0.042
Human U1 snRNP-specific protein A gene	Hs.173522	3.17	0.012
G-rich RNA sequence binding factor 1	Hs.79295	3.16	0.007
Human acidic ribosomal phosphoprotein P0	Hs.136470	2.95	0.003
Homer, neuronal immediate early gene, 2	Hs.93564	2.82	0.017
ribosomal protein S27 (metallopanstimulin 1)	Hs.195453	2.81	0.007
myosin, light polypeptide 3, alkali; ventricular, skeletal, slow	Hs.1815	2.81	0.012
zinc finger protein homologous to Zfp103 in mouse	Hs.155968	2.72	0.007
ribosomal protein S23	Hs.120980	2.72	0.022
ribosomal protein S15a	Hs.2953	2.71	0.010
ribosomal protein S25	Hs.113029	2.70	0.017
ribosomal protein S23	Hs.120980	2.68	0.011
ribosomal protein L35a	Hs.179666	2.65	0.013
cytochrome c oxidase subunit VIIb	Hs.75752	2.65	0.005
ribosomal protein S19	Hs.126701	2.62	0.003
eukaryotic translation initiation factor 3, subunit 9 (eta, 116kD)	Hs.57783	2.61	0.001
ubiquitin A-52 residue ribosomal protein fusion product 1	Hs.119502	2.60	0.005
ribosomal protein L11	Hs.179943	2.55	0.015
tubulin, alpha 2	Hs.98102	2.51	0.049
UDP glycosyltransferase 2 family, polypeptide B15	Hs.183596	0.40	0.000
v-maf musculoaponeurotic fibrosarcoma (avian) oncogene homolog	Hs.266747	0.40	0.000
M phase phosphoprotein 9	Hs.226989	0.40	0.000
patched related protein translocated in renal cancer	Hs.28285	0.39	0.000
Friedreich ataxia region gene X123	Hs.77889	0.39	0.000
zinc finger protein 211	Hs.15110	0.39	0.000
DNA segment, numerous copies, expressed probes (GS1 gene)	Hs.234734	0.39	0.000
Friedreich ataxia	Hs.95998	0.39	0.000
Homo sapiens vav 3 oncogene (VAV3)	Hs.37331	0.39	0.000
zinc finger protein 22 (KOX 15)	Hs.108642	0.39	0.000
eukaryotic translation initiation factor 4E binding protein 2	Hs.151242	0.38	0.000

Homo sapiens RNA cyclase homolog (RNAC)	Hs.113052	0.38	0.000
ADP-ribosyltransferase (NAD+; poly (ADP-ribose) polymerase)-like 1	Hs.77225	0.38	0.000
EGF-like-domain, multiple 5	Hs.5599	0.37	0.000
mutS (E. coli) homolog 5	Hs.257454	0.37	0.000
heterogeneous nuclear protein similar to rat helix destabilizing protein	Hs.249247	0.37	0.000
thyroid hormone receptor-associated protein, 240 kDa subunit	Hs.11861	0.37	0.000
matrix metalloproteinase 16 (membrane-inserted)	Hs.90800	0.36	0.000
ret finger protein-like 3 antisense	Hs.251045	0.36	0.000
zinc finger protein, X-linked	Hs.2074	0.35	0.000
zinc finger protein 273	Hs.89732	0.35	0.000
pleiomorphic adenoma gene 1	Hs.14968	0.35	0.000
C3H-type zinc finger protein; similar to D. melanogaster muscleblind B protein	Hs.266010	0.35	0.000
transcriptional intermediary factor 1	Hs.183858	0.35	0.000
HMBA-inducible	Hs.15299	0.34	0.000
DEAD/H (Asp-Glu-Ala-Asp/His) box polypeptide 16	Hs.266143	0.33	0.000
chromodomain helicase DNA binding protein 2	Hs.36787	0.33	0.001
fucosyltransferase 2 (secretor status included)	Hs.46328	0.33	0.000
survival of motor neuron protein interacting protein 1	Hs.102456	0.33	0.000
CBF1 interacting corepressor	Hs.89421	0.32	0.000
Human translation initiation factor eIF-2alpha mRNA, 3'UTR	Hs.266313	0.32	0.000
Homo sapiens zinc-fingers and homeoboxes 1 (ZHX1), mRNA	Hs.12940	0.32	0.000
GTP cyclohydrolase 1 (dopa-responsive dystonia)	Hs.86724	0.31	0.000
homeo box A2	Hs.58116	0.31	0.000
cAMP responsive element binding protein 1	Hs.79194	0.31	0.000
cofactor required for Sp1 transcriptional activation, subunit 2 (150kD)	Hs.21586	0.31	0.000
DEAD/H (Asp-Glu-Ala-Asp/His) box polypeptide 21	Hs.266290	0.30	0.000
cyclic nucleotide gated channel alpha 1	Hs.1323	0.29	0.000
glial cells missing (Drosophila) homolog b	Hs.227098	0.27	0.000
M phase phosphoprotein 10 (U3 small nucleolar ribonucleoprotein)	Hs.183418	0.27	0.000
zinc finger protein 23 (KOX 16)	Hs.22182	0.27	0.000
general transcription factor IIIA	Hs.75113	0.27	0.000
ribosomal protein S5 pseudogene 1	Hs.237225	0.25	0.000
Sp2 transcription factor	Hs.77031	0.24	0.000

cAMP responsive element binding protein-like 2	Hs.13313	0.21	0.000
nucleophosmin (nucleolar phosphoprotein B23, numatrin)	Hs.173205	0.20	0.000
glycogenin 2	Hs.58589	0.14	0.000

FOC = fold of change; UniGene = accession number in UniGene data bank.

Figure 1:

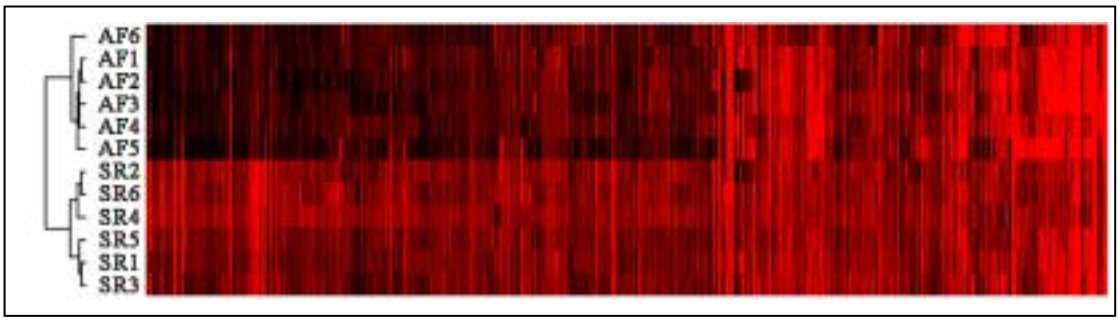

Figure 2:

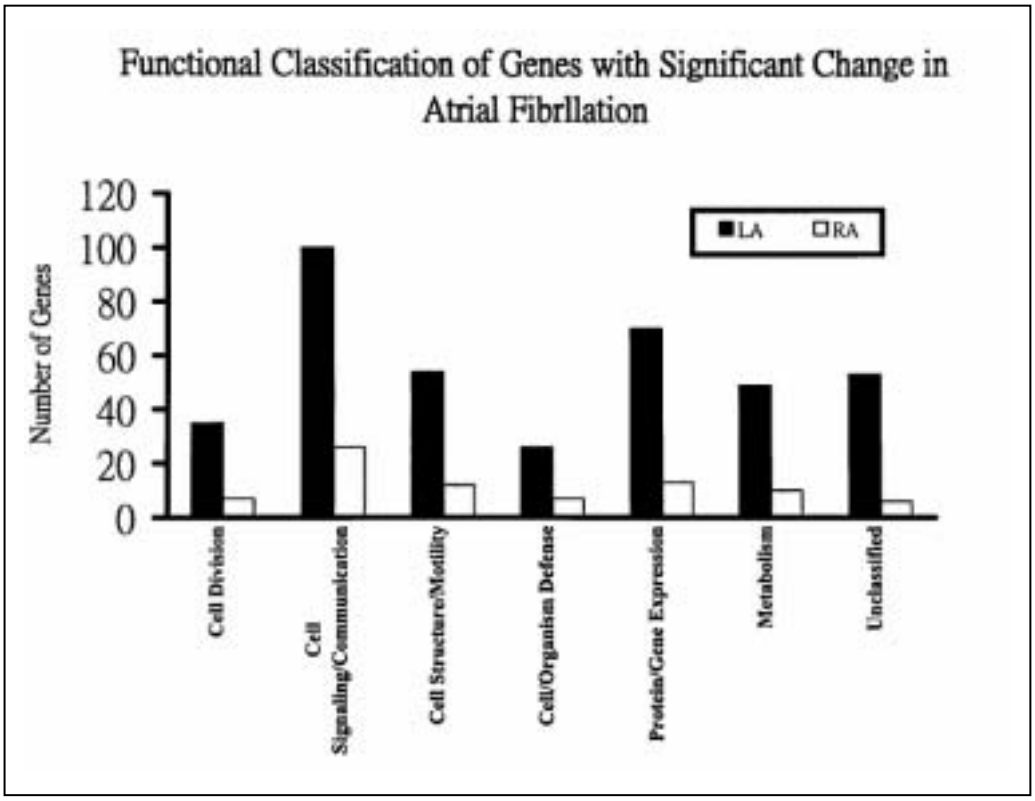

Figure 3:

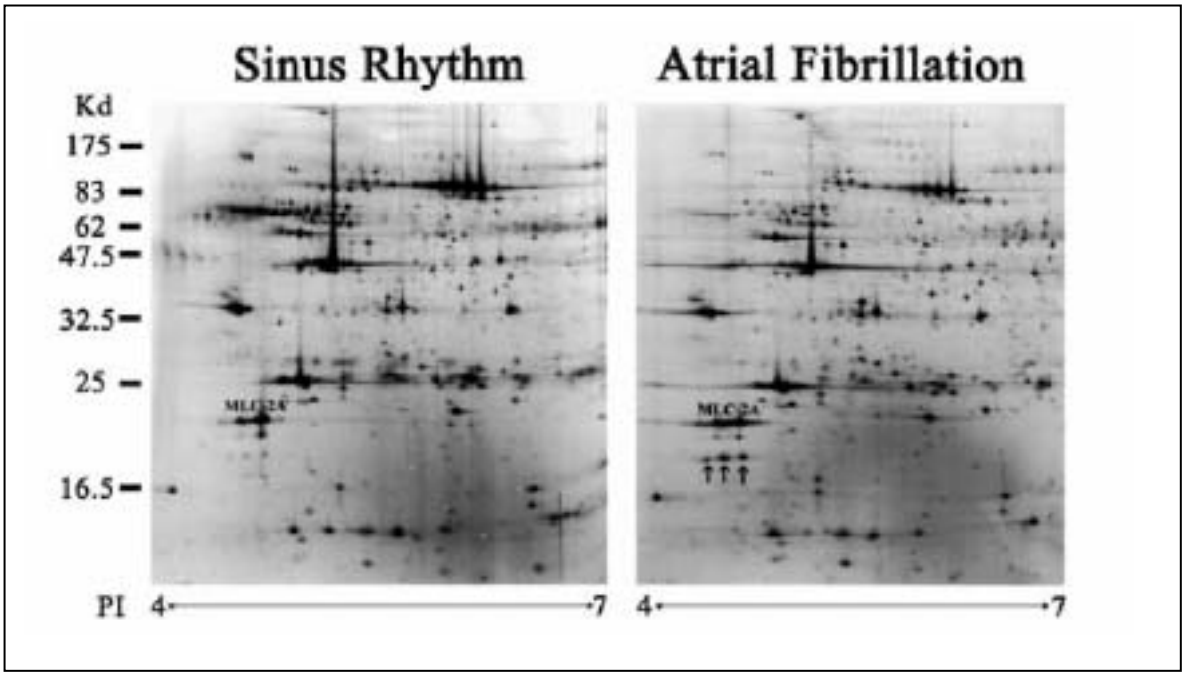

Figure 4: